

ACCOUNTS of CHEMICAL RESEARCH[®]

JUNE 1997

Registered in U.S. Patent and Trademark Office; Copyright 1997 by the American Chemical Society

Making and Breaking the Dioxygen O—O Bond: New Insights from Studies of Synthetic Copper Complexes

WILLIAM B. TOLMAN*

Department of Chemistry and Center for Metals in Biocatalysis, University of Minnesota, 207 Pleasant Street SE, Minneapolis, Minnesota 55455

Received January 8, 1997

Introduction

Dioxygen is a molecule of intrinsic importance in a wide range of biological and industrial processes mediated by metal ions. In nature, aerobic life forms actively transport O₂ from the atmosphere to the appropriate cellular apparatus where the oxidative power of the O—O linkage is garnered for metabolism. The first and seemingly simplest step in this process of respiration involves the reversible coordination of the O₂ molecule to the iron- or copper-containing active sites of the metalloproteins hemoglobin, hemerythrin, and hemocyanin (Hc).¹ This binding step involves electron transfer from the reduced metal site to the O₂ molecule with a concomitant decrease in O—O bond order, as exemplified by the 2-electron reduction of dioxygen to peroxide effected reversibly by the dicopper active site in Hc (Figure 1a).²

William B. Tolman was born on May 20, 1961, in Cleveland, OH. He received a B.A. with University Honors from Wesleyan University (Middletown, CT) in 1983 after learning organometallic chemistry under the tutelage of Alan R. Cutler. His Ph.D. research was performed in the laboratory of K. Peter C. Vollhardt at the University of California, Berkeley. In 1987 he joined the group of Stephen J. Lippard at MIT as a postdoctoral fellow, where he studied model complexes of the active sites of nonheme iron proteins. He became a member of the faculty at the University of Minnesota in 1990 and currently is an Associate Professor of Chemistry. He is the recipient of a Searle Scholars Award, a NSF National Young Investigator Award, and fellowships from the Alfred P. Sloan and Camille & Henry Dreyfus Foundations. Current research in his laboratory is focused on synthetic modeling of copper protein active sites and on developing C₃-symmetric polypyrazolyl ligands for use in stereoselective organometallic chemistry.

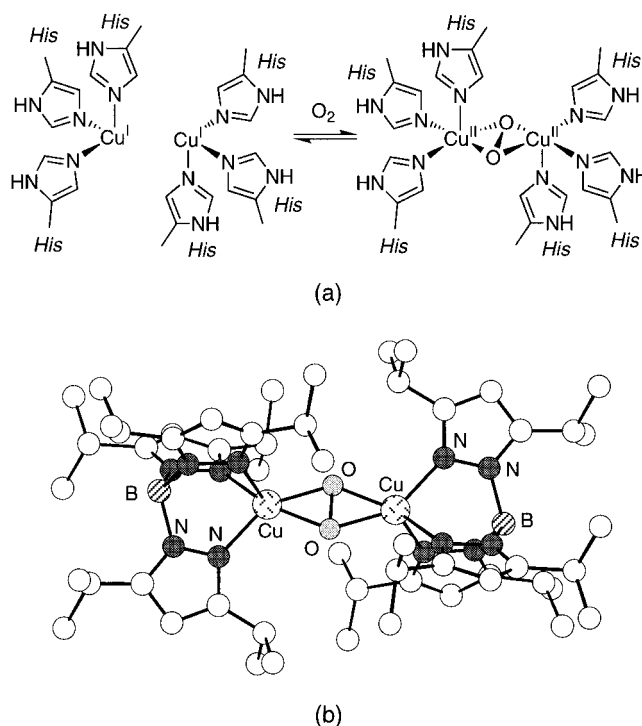


FIGURE 1. (a) Reversible binding of dioxygen to the active site of hemocyanin (Hc) and (b) a drawing of the X-ray crystal structure of the oxyHc model complex [(Tp^{Pr}₂Cu)₂(O₂)] (ref 10; hydrogen atoms not shown for clarity).

In order to function reversibly, further reduction of the peroxide ligand accompanied by O—O bond scission is inhibited in the dioxygen carrier proteins. Such reductive cleavage (i.e., activation) of the O₂ molecule is a fundamental step in metalloenzyme-catalyzed oxidations of organic substrates and oxidase reactions involving the conversion of dioxygen to water.^{3,4} Despite intensive research, questions regarding when and how the O—O bond breaks during oxygenase and oxidase reactions remain largely unanswered, particularly in nonheme systems.^{3–5} Moreover, there is much interest in uncovering the structures and reactivities of the high-valent metalloenzyme intermediates (i.e., metal–oxo species) that form subsequent to O—O bond scission and which in many cases are believed to be responsible for attacking

* E-mail: tolman@chem.umn.edu. Fax: (612) 624-7029.

hydrocarbon substrates during oxygenase reactions.^{3,5,6} High-valent metal–oxo moieties also are implicated in O₂ evolution during photosynthesis. In this fascinating process that constitutes the reverse of dioxygen activation, water molecules are oxidatively coupled to form the O–O bond at a tetranuclear manganese cluster via an unknown mechanism.⁷

Detailed physicochemical and kinetics investigations on synthetic model complexes have contributed greatly to our understanding of dioxygen binding and activation by metal ions in biological and other catalytic systems.⁸ Recent advances in the isolation and characterization of adducts arising from the reaction of Cu(I) complexes with O₂ at low temperature illustrate the utility of this synthetic modeling approach.⁹ Especially notable are the structural and spectroscopic studies of the accurate oxyhemocyanin model complex [(Tp^{IPr₂}Cu)₂(O₂)] [Tp^{IPr₂} = tris(3,5-diisopropylpyrazolyl)hydroborate] performed by Kitajima et al.¹⁰ prior to the solution of the protein X-ray crystal structure^{2a} (Figure 1b). The use of appropriately positioned, large alkyl substituents on the supporting Tp ligand was critical for enabling isolation of the (μ - η^2 : η^2 -peroxy)dicopper complex, as this inhibited through steric influences the more typical reaction of initially formed peroxodicopper

adducts with additional Cu(I) ions to give oxo- or hydroxocopper(II) products and overall 4:1 Cu:O₂ stoichiometries.¹¹

Several years ago my research group and our collaborators began to explore the reactions of dioxygen with Cu(I) complexes supported by 1,4,7-trisubstituted 1,4,7-triazacyclononanes (TACNs),¹² hindered versions of the well-known facially coordinating, tridentate parent TACN.¹³ In the course of these studies we discovered another example of a (μ - η^2 : η^2 -peroxy)dicopper(II) complex as well as an isomer, identified as a new type of intermediate in copper–dioxygen chemistry with a bis(μ -oxo)dicopper(III) core. Moreover, we established that the two isomeric cores can interconvert, thus illustrating reversible scission and formation of the dioxygen O–O bond in a binuclear metal complex. These observations provide the first experimental precedence for the operation of analogous events in reactions of metalloproteins. We also found that the bis(μ -oxo)dicopper compounds are thermally unstable and decompose by cleaving a ligand appendage in a N-dealkylation reaction that models the behavior of monooxygenase enzymes; comprehension of the rate-determining C–H bond activation step was obtained through mechanistic studies. More recently, we have investigated how variation of ligand topology affects the course of Cu(I) complex oxygenation reactions and perturbs the structure and reactivity of the bis(μ -oxo)dicopper unit. In this Account I summarize these findings, which together have provided new insights into the fundamental chemistry of dioxygen activation and generation in biology.

Characterization of Peroxo- and Bis(μ -oxo)-dicopper Complexes

In initial experiments, the Cu(I) complexes [L^{IPr₃}Cu(CH₃CN)]X (L^{IPr₃} = 1,4,7-triisopropyl-1,4,7-triazacyclononane,¹ X = a variety of counterions), which we had prepared originally for use in studies of nitrogen oxide activation,¹⁴ were treated with O₂ at –80 °C in CH₂Cl₂ (Scheme 1, top).¹⁵ The rapidly generated products were identified as [(L^{IPr₃}Cu)₂(μ - η^2 : η^2 -O₂)]X₂ on the basis of 2:1 Cu:O₂ stoichiometries and spectroscopic properties that are analogous to those of oxyhemocyanin^{2b,3h} and Kitajima's crystallographically characterized complex.¹⁰ Specifically, the new compounds are EPR silent due to strong antiferromagnetic coupling between the Cu(II) ions and exhibit features in optical absorption (Figure 2) and resonance Raman [$\nu_{\text{O-O}} = 722 \text{ cm}^{-1}$; $\Delta\nu(^{18}\text{O}_2) = 42 \text{ cm}^{-1}$] spectra diagnostic for the [Cu₂(μ - η^2 : η^2 -O₂)]²⁺ core. Unlike the case for the compound

- (1) Abbreviations used: B(Ar)₄[–] = B[(CF₃)₂C₆H₃]₄[–]; Hc = hemocyanin; HOMO = highest occupied molecular orbital; *i*-Pr₄dtne = 1,2-bis-(4,7-diisopropyl-1,4,7-triazacyclononane)-1-cyclononyl)ethane; LUMO = lowest unoccupied molecular orbital; L^{Bn₃} = 1,4,7-tribenzyl-1,4,7-triazacyclononane; L^{IPr₃} = 1,4,7-triisopropyl-1,4,7-triazacyclononane; oxyHc = oxyhemocyanin; oxyTyr = oxytyrosinase; TACN = 1,4,7-triazacyclononane; Tp = trispyrazolylhydroborate; Tp^{RR'} = tris(3-R,5-R'-pyrazolyl)hydroborate; Tyr = tyrosinase.
- (2) (a) Magnus, K. A.; Ton-That, H.; Carpenter, J. E. *Chem. Rev.* **1994**, *94*, 727–735. (b) Solomon, E. I.; Tuzcek, F.; Root, D. E.; Brown, C. A. *Chem. Rev.* **1994**, *94*, 827–856.
- (3) Lead references for selected examples of metalloxygenases. Cytochrome P450 (heme-Fe): (a) *Cytochrome P-450: Structure, Mechanism, and Biochemistry*, 2nd ed.; Ortiz de Montellano, P. R., Ed.; Plenum Press: New York, 1995. (b) Sono, M.; Roach, M. P.; Coulter, E. D.; Dawson, J. H. *Chem. Rev.* **1996**, *96*, 2841–2887. Methane monooxygenase and ribonucleotide reductase (nonheme Fe): (c) Lipscomb, J. D. *Annu. Rev. Microbiol.* **1994**, *48*, 371–399. (d) Stubbe, J. *Adv. Enzymol.* **1990**, *63*, 349–419. (e) Fontecave, M.; Nordlund, P.; Eklund, H.; Reichard, P. *Adv. Enzymol.* **1992**, *65*, 147–183. Dopamine β -monooxygenase and peptidylglycine α -amidating monooxygenase (Cu): (f) Klinman, J. P. *Chem. Rev.* **1996**, *96*, 2541–2561. Tyrosinase (Cu): (g) Sánchez-Ferrer, A.; Rodríguez-López, J. N.; García-Cánovas, F.; García-Carmona, F. *Biochim. Biophys. Acta* **1995**, *1247*, 1–11. (h) Solomon, E. I.; Sundaram, U. M.; Machonkin, T. E. *Chem. Rev.* **1996**, *96*, 2563–2605. See also ref 2b.
- (4) Oxidases: (a) Babcock, G. T.; Wikström, M. *Nature* **1992**, *356*, 301–309. (b) Messerschmidt, A. *Adv. Inorg. Chem.* **1994**, *40*, 121–185. (c) Ferguson-Miller, S.; Babcock, G. T. *Chem. Rev.* **1996**, *96*, 2889–2907.
- (5) (a) Feig, A. L.; Lippard, S. J. *Chem. Rev.* **1994**, *94*, 759–805. (b) Wallar, B. J.; Lipscomb, J. D. *Chem. Rev.* **1996**, *96*, 2625–2657.
- (6) (a) Que, L., Jr.; Dong, Y. *Acc. Chem. Res.* **1996**, *29*, 190–196. (b) Sturgeon, B. E.; Burdi, D.; Chen, S.; Huynh, B.-H.; Edmondson, D. E.; Stubbe, J.; Hoffman, B. M. *J. Am. Chem. Soc.* **1996**, *118*, 7551–7557.
- (7) (a) Yachandra, V. K.; Sauer, K.; Klein, M. P. *Chem. Rev.* **1996**, *96*, 2927–2950. (b) *Manganese Redox Enzymes*; Pecoraro, V. L., Ed.; VCH: New York, 1992.
- (8) Karlin, K. D. *Science* **1993**, *261*, 701–708.
- (9) Reviews: (a) Karlin, K. D.; Gultneh, Y. *Prog. Inorg. Chem.* **1987**, *35*, 219–328. (b) Sorrell, T. N. *Tetrahedron* **1989**, *40*, 3–68. (c) Tyeklár, Z.; Karlin, K. D. *Acc. Chem. Res.* **1989**, *22*, 241–248. (d) Karlin, K. D.; Tyeklár, Z.; Zuberbühler, A. D. In *Bioinorganic Catalysis*; Reedijk, J., Ed.; Marcel Dekker, Inc.: New York, 1993; pp 261–315. (e) Kitajima, N.; Moro-oka, Y. *Chem. Rev.* **1994**, *94*, 737. (f) Karlin, K. D.; Tyeklár, Z. *Adv. Inorg. Biochem.* **1994**, *9*, 123–172. (g) Fox, S.; Karlin, K. D. In *Active Oxygen in Biochemistry*; Valentine, J. S., Foote, C. S., Greenberg, A., Liebman, J. F., Eds.; Blackie Academic & Professional, Chapman & Hall: Glasgow, Scotland, 1995; pp 188–231. (h) Karlin, K. D.; Kaderli, S.; Zuberbühler, A. D. *Acc. Chem. Res.* **1997**, *30*, 139.
- (10) Kitajima, N.; Fujisawa, K.; Fujimoto, C.; Moro-oka, Y.; Hashimoto, S.; Kitagawa, T.; Toriumi, K.; Tatsumi, K.; Nakamura, A. *J. Am. Chem. Soc.* **1992**, *114*, 1277–1291.

- (11) Davies, G.; El-Sayed, M. A. *Comments Inorg. Chem.* **1985**, *4*, 151–162.
- (12) 1,4,7-Triisopropyl-1,4,7-triazacyclononane: (a) Haselhorst, G.; Stotzel, S.; Strassburger, A.; Walz, W.; Wiegardt, K.; Nuber, B. *J. Chem. Soc., Dalton Trans.* **1993**, 83–90. 1,4,7-Tribenzyl-1,4,7-triazacyclononane: (b) Beissel, T.; Della Vedova, B. S. P. C.; Wiegardt, K.; Boese, R. *Inorg. Chem.* **1990**, *29*, 1736–1741.
- (13) Wiegardt, K.; Chaudhury, P. *Prog. Inorg. Chem.* **1988**, *35*, 329–436.
- (14) (a) Mahapatra, S.; Halfen, J. A.; Tolman, W. B. *J. Chem. Soc., Chem. Commun.* **1994**, 1625–1626. (b) Halfen, J. A.; Mahapatra, S.; Olmstead, M. M.; Tolman, W. B. *J. Am. Chem. Soc.* **1994**, *116*, 2173–2174. (c) Halfen, J. A.; Tolman, W. B. *J. Am. Chem. Soc.* **1994**, *116*, 5475–5476. (d) Halfen, J. A.; Mahapatra, S.; Wilkinson, E. C.; Gengenbach, A. J.; Young, V. G., Jr.; Que, L., Jr.; Tolman, W. B. *J. Am. Chem. Soc.* **1996**, *118*, 763–776.
- (15) Mahapatra, S.; Halfen, J. A.; Wilkinson, E. C.; Que, L., Jr.; Tolman, W. B. *J. Am. Chem. Soc.* **1994**, *116*, 9785–9786.

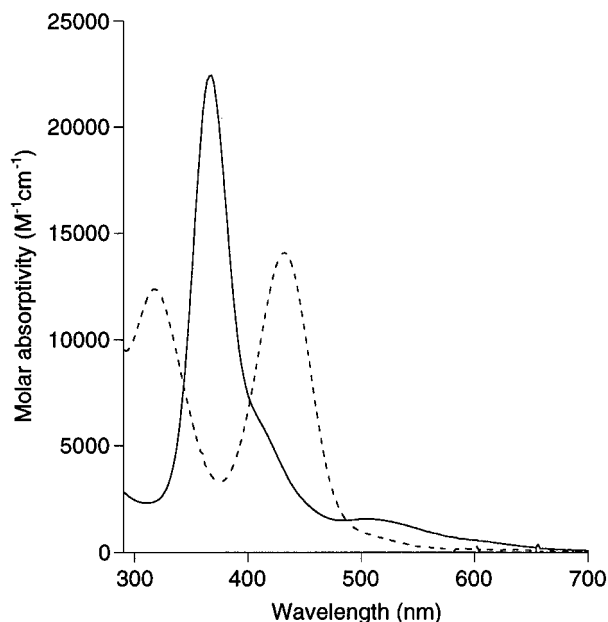
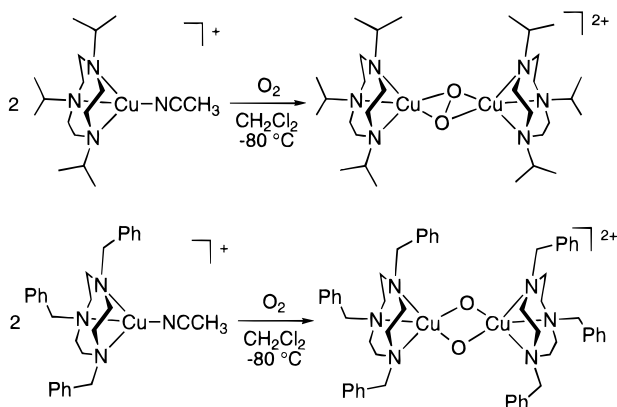


FIGURE 2. Electronic absorption spectra of CH_2Cl_2 solutions (-80°C) of $[(\text{L}^{\text{IPr}_3}\text{Cu})_2(\mu\text{-}\eta^2\text{:}\eta^2\text{-O}_2)](\text{PF}_6)_2$ (—) and $[(\text{L}^{\text{Bn}_3}\text{Cu})_2(\mu\text{-O})_2](\text{SbF}_6)_2$ (---).

Scheme 1



supported by Tp^{IPr_2} , dioxygen binding could be reversed by rapidly warming the solutions of $[(\text{L}^{\text{IPr}_3}\text{Cu})_2(\mu\text{-}\eta^2\text{:}\eta^2\text{-O}_2)]\text{X}_2$ in CH_2Cl_2 under vacuum or while purging with N_2 or Ar. Thus, functional modeling of hemocyanin was achieved, a feat also accomplished concurrently by Kurtz¹⁶ and Sorrell¹⁷ using hindered triimidazolylphosphine supporting ligands.

The first hint that there was more to this chemistry than a straightforward replication/extension of Kitajima's original findings came from preliminary results of low-temperature X-ray structural studies on crystals grown from CH_2Cl_2 solutions stored at -80°C .¹⁸ Three separate data sets were collected, and two were solved successfully ($\text{X} = \text{PF}_6^-$), both of which showed the presence of two crystallographically independent half-dimers in the asymmetric unit (space group $P\bar{1}$). Expansion by an inversion operation revealed two binuclear complexes in which two oxygen atoms lie between each dicopper pair, with reasonable thermal parameters for all atoms (one mol-

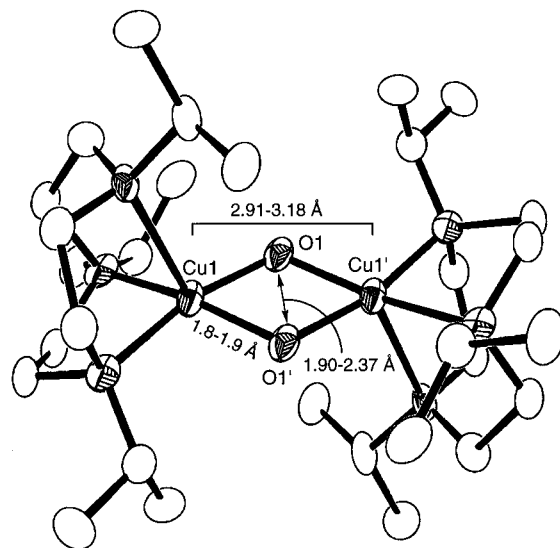


FIGURE 3. Drawing of one of the two independent binuclear species in one of the X-ray structures of crystals isolated from the reaction of $[(\text{L}^{\text{IPr}_3}\text{Cu})(\text{CH}_3\text{CN})]\text{PF}_6$ with O_2 in CH_2Cl_2 . The indicated ranges of interatomic distances encompass those observed in the four molecules from the two solved structures.

ecule shown in Figure 3). However, the geometric parameters of the four $[\text{Cu}_2\text{O}_2]^{2+}$ units significantly differ from each other (cf. ranges of interatomic distances indicated in Figure 3), and in no instance are they consistent with a $(\mu\text{-}\eta^2\text{:}\eta^2\text{-peroxo})\text{dicopper(II)}$ formulation ($\text{Cu}\cdots\text{Cu} \approx 3.6 \text{ \AA}$, $\text{O}\text{-O} \approx 1.4 \text{ \AA}$).¹⁰ The topological variations among the four $[\text{Cu}_2\text{O}_2]^{2+}$ cores were particularly troubling, suggesting the possible existence of some kind of compositional disorder akin to that delineated by Parkin for supposed "bond stretch isomers",¹⁹ here involving the peroxo compound and another, unidentified species.²⁰

In an effort to change the crystal packing and unravel the apparent anomalies found in the X-ray structures, we changed the supporting ligand to one with benzyl groups in place of the isopropyl substituents. We then prepared the analogous Cu(I) starting materials $[(\text{L}^{\text{Bn}_3}\text{Cu})(\text{CH}_3\text{CN})]\text{X}$ ($\text{L}^{\text{Bn}_3} = 1,4,7\text{-tribenzyl-1,4,7-triazacyclononane}$) and attempted to repeat the low-temperature oxygenation chemistry. On the basis of initially observed solution spectral features and, ultimately, complete characterization by both solution and solid state spectroscopic and crystallographic methods,²¹ the product of this oxygenation reaction was identified not as the anticipated $(\mu\text{-}\eta^2\text{:}\eta^2\text{-peroxo})\text{dicopper(II)}$ complex, but rather as $[(\text{L}^{\text{Bn}_3}\text{Cu})_2(\mu\text{-O})_2]\text{X}_2$, a novel high-valent molecule in copper–dioxygen chemistry (Scheme 1, bottom).

Several observations led to our initial hypothesis of the $[\text{Cu}_2(\mu\text{-O})_2]^{2+}$ core in the new compound. Manometric

(19) (a) Parkin, G. *Acc. Chem. Res.* **1992**, *25*, 455–460. (b) Parkin, G. *Chem. Rev.* **1993**, *93*, 887–911.

(20) In support of this notion, resonance Raman analysis of a polycrystalline sample of the BPh_4^- salt prepared with $^{18}\text{O}_2$ revealed a $\nu_{\text{O-O}}$ at 680 cm^{-1} . This result is consistent with the presence of a $(\mu\text{-}\eta^2\text{:}\eta^2\text{-peroxo})\text{dicopper(II)}$ unit in the crystals that would be expected to exhibit an O–O bond distance of $\sim 1.4 \text{ \AA}$.

(21) (a) Mahapatra, S.; Halfen, J. A.; Wilkinson, E. C.; Pan, G.; Cramer, C. J.; Que, L., Jr.; Tolman, W. B. *J. Am. Chem. Soc.* **1995**, *117*, 8865–8866. (b) Halfen, J. A.; Mahapatra, S.; Wilkinson, E. C.; Kaderli, S.; Young, V. G., Jr.; Que, L., Jr.; Zuberbühler, A. D.; Tolman, W. B. *Science* **1996**, *271*, 1397–1400. (c) Mahapatra, S.; Halfen, J. A.; Wilkinson, E. C.; Pan, G.; Wang, X.; Young, V. G., Jr.; Cramer, C. J.; Que, L., Jr.; Tolman, W. B. *J. Am. Chem. Soc.* **1996**, *118*, 11555–11574.

(16) Lynch, W. E.; Kurtz, D. M., Jr.; Wang, S.; Scott, R. A. *J. Am. Chem. Soc.* **1994**, *116*, 11030–11038.

(17) Sorrell, T. N.; Allen, W. E.; White, P. S. *Inorg. Chem.* **1995**, *34*, 952–960.

(18) Halfen, J. A.; Olmstead, M. M.; Tolman, W. B. Unpublished results.

measurements of dioxygen uptake by the Cu(I) starting material in CH_2Cl_2 at -80°C showed a 2:1 Cu: O_2 stoichiometry. The formula of the product was corroborated by low-temperature electrospray ionization mass spectrometry. Solutions of the complex are EPR silent and exhibit sharp ^1H NMR spectra in the 0–10 ppm region, indicative of a diamagnetic ($S = 0$) ground state. Taken together, the dioxygen uptake, mass spectral, and NMR data may be interpreted to support either a bis(μ -oxo)- or peroxodicopper structure. However, we observed intense features in UV–vis absorption spectra that differed significantly from those characteristic of the $[\text{Cu}_2(\mu\text{-}\eta^2\text{:}\eta^2\text{-O}_2)]^{2+}$ core (Figure 2). Furthermore, in the resonance Raman spectrum ($\lambda_{\text{ex}} = 457.9$ nm) two peaks were found at 602 and 612 cm^{-1} that shifted to a single peak at 583 cm^{-1} when the compound was prepared with $^{18}\text{O}_2$. These features cannot be attributed to a peroxide ligand on the basis of their low energies, well outside the range for transition metal peroxo compounds ($720\text{--}900\text{ cm}^{-1}$), and the small magnitude of the ^{18}O isotope shift ($\sim 24\text{ cm}^{-1}$), approximately half of that observed for the $[\text{Cu}_2(\mu\text{-}\eta^2\text{:}\eta^2\text{-O}_2)]^{2+}$ unit. Instead, we assign the Raman bands as a symmetric vibration of the $[\text{Cu}_2(\mu\text{-O})_2]^{2+}$ core, split into a Fermi doublet in the $^{16}\text{O}_2$ case. This assignment is supported by (i) depolarization ratio data consistent with a symmetric vibration, (ii) the good agreement of the observed ^{18}O isotope shift to that expected for a Cu–O harmonic oscillator (28 cm^{-1}) and to that calculated theoretically for a $[\text{Cu}_2(\mu\text{-O})_2]^{2+}$ rhomb [$\nu(^{16}\text{O}) = 630\text{ cm}^{-1}$, $\Delta(^{18}\text{O}) = 29\text{ cm}^{-1}$, *vide infra*],^{21c} and (iii) the presence of analogous features at $660\text{--}700\text{ cm}^{-1}$ identified for complexes comprised of $[\text{M}_2(\mu\text{-O})_2]^{2+}$ cores (M = Fe or Mn).²² Finally, the EXAFS spectrum of a solid sample contains a prominent second-shell feature that was fit to a Cu–Cu distance of 2.86 \AA , similar to that seen in other $[\text{M}_2(\mu\text{-O})_2]^{n+}$ units^{7a,22,23} but much shorter than that in the $[\text{Cu}_2(\mu\text{-}\eta^2\text{:}\eta^2\text{-O}_2)]^{2+}$ core ($\sim 3.6\text{ \AA}$).

A low-temperature X-ray crystal structure of the $\text{L}^{\text{Bn}_3\text{-}d_{21}}$ (benzyl groups perdeuterated) complex provided conclusive proof of the nature of the new species and corroborated our interpretations of the spectroscopic evidence (Figure 4). Notable geometric parameters include Cu \cdots Cu and Cu–O distances of $2.794(2)$ and 1.81 (av) \AA , respectively, that are significantly shorter than the analogous distances in more commonly encountered bis(μ -hydroxo)dicopper(II) cores (~ 3.00 and 1.95 \AA).^{21c,24} The short Cu–O distances implicate a *formal* copper oxidation state of +III, an assignment which is supported by a bond valence sum analysis^{21c,25} and close agreement between the core topology of the complex with that of the extended

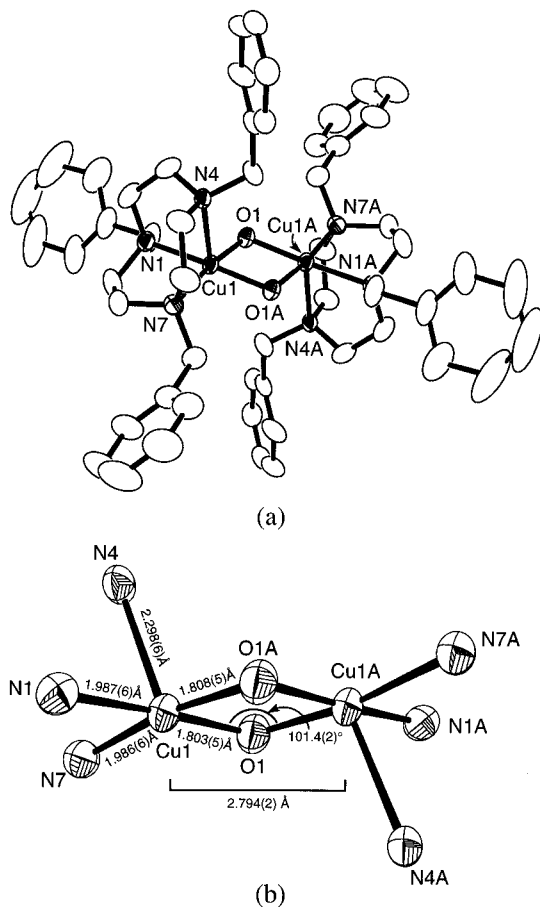


FIGURE 4. (a) X-ray crystal structure of the cationic portion of $[(\text{L}^{\text{Bn}_3\text{-}d_{21}}\text{Cu})_2(\mu\text{-O})_2](\text{SbF}_6)_2$ and (b) a view of the copper coordination sphere labeled with selected interatomic distances and bond angles.

solid KCuO_2 (Cu \cdots Cu = 2.71 \AA , Cu–O = 1.84 \AA , Cu–O–Cu = 95°).²⁶ These core geometries are also highly congruent with those of high oxidation state bis(μ -oxo)-diiron^{6a,27} and -dimanganese²⁸ complexes; this and other aspects of the interesting correspondence among these “diamond” cores in synthetic compounds and metalloprotein active sites that contain Cu, Fe, and Mn are explored in more detail elsewhere.²⁹ Short Cu–O distances of 1.83 \AA also have been cited in support of a +III oxidation state assignment for the unique copper ion in the novel oxo-capped cluster $[\text{L}_3\text{Cu}_3(\text{O})_2]^{3+}$ [Figure 5; L = *N,N,N,N'*-tetramethyl-(1*R*,2*R*)-cyclohexanediamine].³⁰ This compound also is derived from the reaction of a Cu(I) precursor with O_2 at low temperature, but in an unusual 3:1 Cu: O_2 stoichiometry. An additional feature of the X-ray structure of the bis(μ -oxo)dicopper complex that has potential relevance to its reactivity is the presence of close contacts between the bridging oxo groups and several benzylic C–D bonds [D \cdots O distances are $\sim 2.3\text{ \AA}$].^{21c} As described below, these C–D(H) bonds are cleaved during the decomposition of the bis(μ -oxo)dicopper compounds

(22) Dong, Y.; Fujii, H.; Hendrich, M. P.; Leising, R. A.; Pan, G.; Randall, C. R.; Wilkinson, E. C.; Zang, Y.; Que, L., Jr.; Fox, B. G.; Kauffmann, K.; Münck, E. *J. Am. Chem. Soc.* **1995**, *117*, 2778–2792 and references cited therein.

(23) For recent biological Mn examples, see: (a) DeRose, V. J.; Mukerji, I.; Latimer, M. J.; Yachandra, V. K.; Sauer, K.; Klein, M. P. *J. Am. Chem. Soc.* **1994**, *116*, 5239–5249. (b) Riggs-Gelasco, P. J.; Mei, R.; Yocum, C. F.; Penner-Hahn, J. E. *J. Am. Chem. Soc.* **1996**, *118*, 2387–2399.

(24) (a) Lee, S. C.; Holm, R. H. *Inorg. Chem.* **1993**, *32*, 4745–4753 and references cited therein. (b) Hodgson, D. J. *Prog. Inorg. Chem.* **1975**, *19*, 173–242. (c) Kitajima, N.; Hikichi, S.; Tanaka, M.; Moro-oka, Y. *J. Am. Chem. Soc.* **1993**, *115*, 5496–5508.

(25) (a) Brown, I. D.; Altermatt, D. *Acta Crystallogr.* **1985**, *B41*, 244–247. (b) Thorp, H. H. *Inorg. Chem.* **1992**, *31*, 1585–1588. (c) Hati, S.; Datta, D. *J. Chem. Soc., Dalton Trans.* **1995**, 1177–1182.

(26) Hestermann, K.; Hoppe, R. *Z. Anorg. Allg. Chem.* **1969**, *367*, 249–269.

(27) Shu, L.; Nesheim, J. C.; Kauffmann, K.; Münck, E.; Lipscomb, J. D.; Que, L., Jr. *Science* **1997**, *275*, 515–518.

(28) (a) Wiegardt, K. *Angew. Chem., Int. Ed Engl.* **1989**, *28*, 1153–1172. (b) Manchanda, R.; Brudvig, G. W.; Crabtree, R. H. *Coord. Chem. Rev.* **1995**, *144*, 1–38.

(29) Que, L., Jr.; Tolman, W. B. Manuscript in preparation.

(30) Cole, A. P.; Root, D. E.; Mukherjee, P.; Solomon, E. I.; Stack, T. D. P. *Science* **1996**, *273*, 1848–1850.

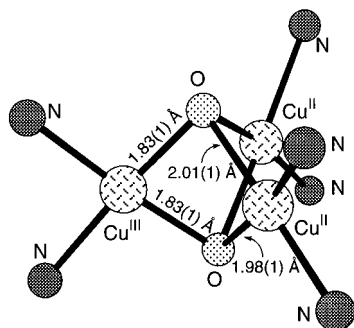


FIGURE 5. Drawing of the copper coordination spheres of $[\text{L}_3\text{Cu}_3(\text{O})_2]^{3+}$ from the reported X-ray crystallographic coordinates [ref 30; L = *N,N,N,N'*-tetramethyl-(1*R*,2*R*)-cyclohexanediamine].

by a mechanism involving direct attack by the electrophilic oxo bridges.³¹ Thus, one may view the C–D···O interactions in the X-ray structure as starting points on the decomposition reaction trajectory.

A more complete view of the electronic structure of the $[\text{Cu}_2(\mu\text{-O})_2]^{2+}$ core was revealed by *ab initio* theory.^{21c,32} Using the X-ray crystallographic coordinates as a starting point, restricted Hartree–Fock (RHF) calculations (STO-3G basis set) performed on the model $\{[(\text{NH}_3)_3\text{Cu}]_2(\mu\text{-O})_2\}^{2+}$ converged to a structure highly congruent with that observed experimentally; calculated (experimental) distances and angles are Cu–Cu = 2.734 Å (2.794 Å), Cu–O = 1.78 Å (1.81 Å), and Cu–O–Cu = 100.3° (101.4°). The finding of a closed-shell singlet ground state at more complete levels of electronic structure theory corroborates the observed EPR silence and sharp NMR spectral properties of the synthetic compound. Moreover, analytic frequency calculations yielded $\nu(^{16}\text{O})$ and $\nu(^{18}\text{O})$ values for the symmetric Cu_2O_2 breathing vibration in good agreement with the experimentally determined Raman spectroscopic data (*vide supra*). Various calculations were then performed which led to the conclusion that $\{[(\text{NH}_3)_3\text{Cu}]_2(\mu\text{-O})_2\}^{2+}$ is best described by a multiconfigurational wave function wherein significant population of the doubly excited state $\text{LUMO}^2 \leftarrow \text{HOMO}^2$ as well as smaller contributions from other states augment the overall ground state. The atomic orbital interactions that comprise the calculated frontier molecular orbitals are shown in Figure 6. A notable feature of the HOMO is the strong bonding interaction between the copper $d_{x^2-y^2}$ and oxygen p orbitals, the latter of which are antibonding with respect to each other (i.e., the $d_{x^2-y^2}$ orbitals combine in a bonding fashion with the O–O σ^* orbital). This extensive overlap of dioxygen σ^* and copper orbitals contrasts with the analogous, yet significantly weaker, interaction seen for the $(\mu\text{-}\eta^2\text{:}\eta^2\text{-peroxo})\text{dicopper}$ core in which the O–O bond is retained (*vide infra*).^{2b,33} Moreover, it implies that the bis($\mu\text{-oxo}$)dicopper unit is characterized by a high degree of Cu–O covalency and that there is significant removal of charge from the copper atoms onto the oxygen atoms, consistent with the formal $[\text{Cu}^{\text{III}}_2(\mu\text{-O}^{2-})_2]^{2+}$ oxidation state description.

Both the LUMO and LUMO + 1 are formed from copper $d_{x^2-y^2}$ and oxygen p orbitals that are net antibonding between all the atoms. Further discussion of these low-lying acceptor orbitals will be deferred, the LUMO + 1 being of particular interest to the discussion below because it rationalizes the observed electrophilic reactivity of the experimental systems.

Interconversion of the Isomeric Peroxo- and Bis($\mu\text{-oxo}$)dicopper Cores

At this point in our studies we had observed that the nature of the oxygenation product depended on the identity of the TACN ligand substituents; isopropyl groups (L^{iPr_3}) favored the $\mu\text{-}\eta^2\text{:}\eta^2\text{-peroxo}$ mode while benzyl groups (L^{Bn_3}) favored the bis($\mu\text{-oxo}$) structure. With the identification of the latter species, however, our attention turned back to the confusing results of the X-ray diffraction experiments on the crystals obtained from solutions of the peroxo compound supported by L^{iPr_3} . It was at this juncture that it occurred to us that the “contaminating” species in these crystals might be a bis($\mu\text{-oxo}$) isomer, whose contracted core topology would explain the Cu···Cu and Cu–O distances observed to be shorter than those expected for the $\mu\text{-}\eta^2\text{:}\eta^2\text{-peroxo}$ structure. Unfortunately, attempts to construct a reliable compositional disorder model of the crystallographic data have not been successful to date, in large part because of the complexity of the problem involving positional displacements of no fewer than 40 atoms. On the basis of several additional experimental results, however, we concluded that a bis($\mu\text{-oxo}$)dicopper complex capped by L^{iPr_3} was accessible and, even more startling, that it and its isomer $[(\text{L}^{\text{iPr}_3}\text{Cu})_2(\mu\text{-}\eta^2\text{:}\eta^2\text{-O}_2)]^{2+}$ could interconvert.^{21b}

First, we found that oxygenation of $[\text{L}^{\text{iPr}_3}\text{Cu}(\text{CH}_3\text{CN})\text{X}]$ ($\text{X} = \text{PF}_6^-$ or ClO_4^-) in THF at low temperature did not afford the peroxo adduct (as when the reaction was carried out in CH_2Cl_2), but instead generated a bis($\mu\text{-oxo}$) isomer, which was identified by manometry (2:1 Cu:O₂) and the congruence of its UV–vis [$\lambda_{\text{max}} = 324$ ($\epsilon = 10\,100\text{ M}^{-1}\text{ cm}^{-1}$), 448 (13 000 nm)] and resonance Raman [$\nu = 600\text{ cm}^{-1}$; $\Delta\nu(^{18}\text{O}_2) = 20\text{ cm}^{-1}$] spectral properties with those of $[(\text{L}^{\text{Bn}_3}\text{Cu})_2(\mu\text{-O})_2]\text{X}_2$. In a further corroboration of the assignment of the product as $[(\text{L}^{\text{iPr}_3}\text{Cu})_2(\mu\text{-O})_2]\text{X}_2$, the EXAFS spectrum collected on the solid precipitated from THF (fit with Cu···Cu = 2.88 Å) also was quite similar to that obtained for the L^{Bn_3} -supported complex.^{21c} Interestingly, when the oxygenation was performed in acetone (any counterion) or when counterions other than PF_6^- or ClO_4^- were used in THF ($\text{X} = \text{SbF}_6^-$, BPh_4^- , $\text{B}(\text{Ar})_4^-$),¹ mixtures of the L^{iPr_3} -capped peroxo and bis($\mu\text{-oxo}$) compounds were produced, as indicated by the presence of both of their respective UV–vis and Raman spectroscopic signatures.

Second, stopped-flow experiments in which the evolution of the ~4:1 peroxo/bis($\mu\text{-oxo}$) mixture from $[\text{L}^{\text{iPr}_3}\text{Cu}(\text{CH}_3\text{CN})]\text{SbF}_6$ and O₂ in acetone was monitored by UV–vis spectroscopy between –83 and –50 °C revealed a first-order dependence of the reaction rate on the concentration of the starting Cu(I) compound.^{21b} Significantly, rate constants for the formation of each product are identical at all temperatures [at –60 °C, $k(\text{peroxo}) = k(\text{bisoxo}) =$

(31) Mahapatra, S.; Halfen, J. A.; Tolman, W. B. *J. Am. Chem. Soc.* **1996**, *118*, 11575–11586.

(32) Cramer, C. J.; Smith, B. A.; Tolman, W. B. *J. Am. Chem. Soc.* **1996**, *118*, 11283–11287.

(33) Baldwin, M. J.; Root, D. E.; Pate, J. E.; Fujisawa, K.; Kitajima, N.; Solomon, E. I. *J. Am. Chem. Soc.* **1992**, *114*, 10421–10431.

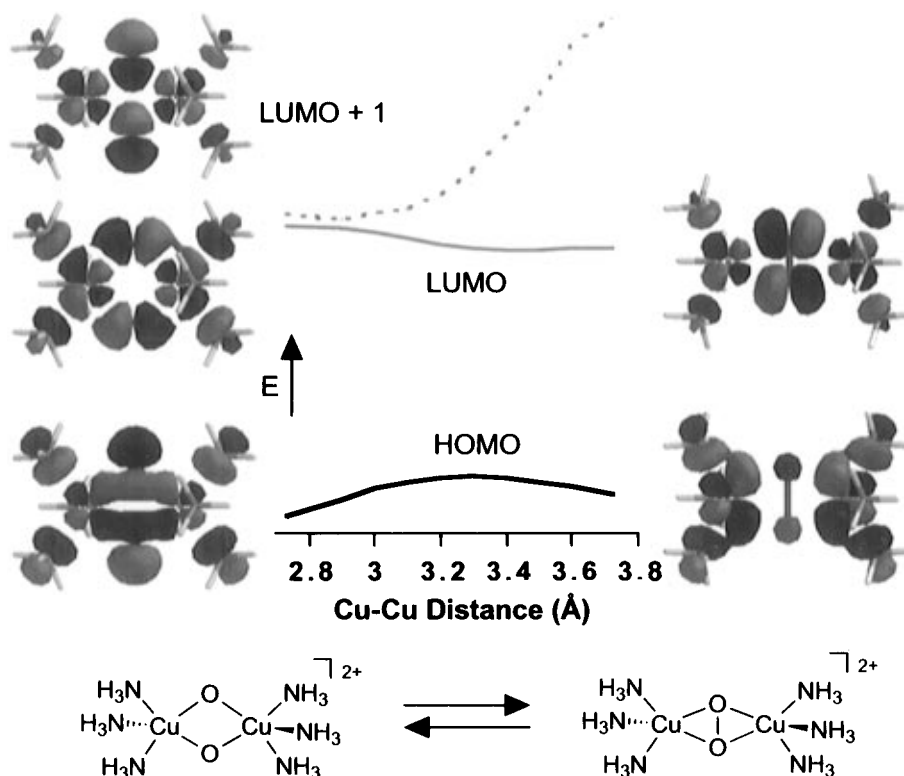
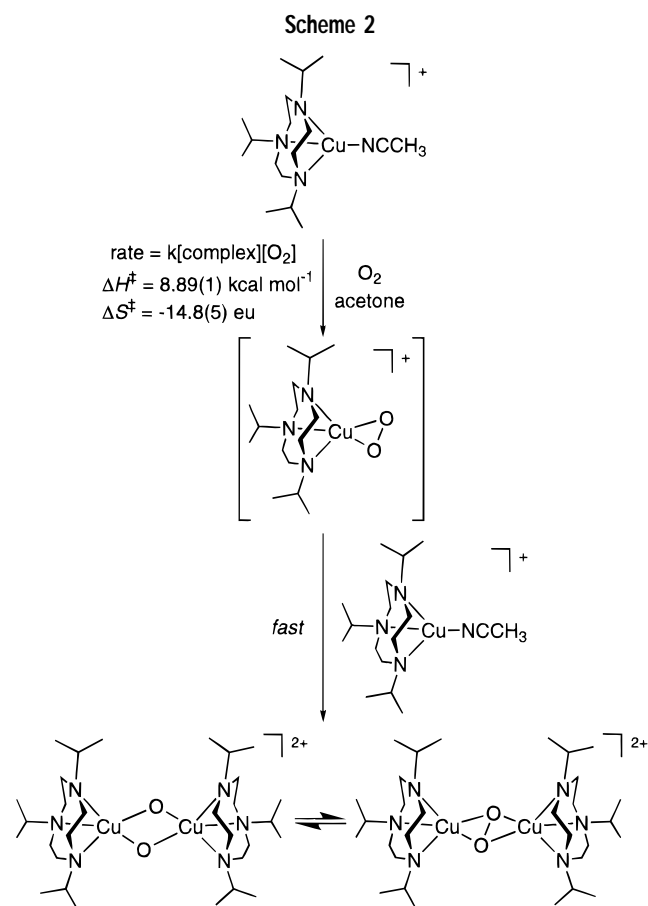


FIGURE 6. Calculated Walsh diagram showing selected frontier molecular orbitals and their relative energies during the interconversion of $\{[(\text{NH}_3)_3\text{Cu}]_2(\mu\text{-O})_2\}^{2+}$ (left) and $\{[(\text{NH}_3)_3\text{Cu}]_2(\mu\text{-}\eta^2\text{:}\eta^2\text{-O}_2)\}^{2+}$ (right) (ref 32).



$1.77 \text{ M}^{-1} \text{ s}^{-1}$. These results are consistent with generation of a mononuclear O_2 adduct (a mononuclear superoxo complex) in the rate-determining step (Scheme 2). Activation parameters similar to those previously observed for

the formation of $[(\text{BQPA})\text{CuO}_2]^+$ [BQPA = bis(2-quinolyl)-(2-pyridylmethyl)amine]³⁴ provide further support for this hypothesis. Both the subsequent trapping by a second Cu(I) species and, most importantly, equilibration between the peroxo and bis(μ -oxo) isomers must be more rapid than the initial adduct formation to explain the equality of the formation rate constants for each isomer at each temperature.

Finally, in addition to this kinetic evidence in favor of equilibration of the peroxo and bis(μ -oxo) compounds in acetone solution, we discovered that each species could be quantitatively converted to the other by interchanging CH_2Cl_2 and THF solvents. Thus, >10-fold dilution of a CH_2Cl_2 solution of the peroxo complex (ClO_4^- salt) at -80°C with THF caused its transformation to the bis(μ -oxo) isomer. Moreover, a similar dilution of a THF solution of the bis(μ -oxo) complex with CH_2Cl_2 converted it to the peroxo form. The involvement of mononuclear intermediates or free O_2 in these processes appears unlikely on the basis of the results of two control experiments.³¹ When $[(\text{L}^{\text{Bn}_3}\text{-d}_{21}\text{-Cu})_2(\mu\text{-O})_2](\text{ClO}_4)_2$ and $[(\text{L}^{\text{IPr}_3}\text{-d}_{21}\text{-Cu})_2(\mu\text{-O})_2](\text{ClO}_4)_2$ were mixed in THF at -80°C and the solution composition was monitored by electrospray ionization mass spectrometry at -40°C , only the starting material $[\text{M} - \text{ClO}_4]^+$ parent ions and none of the crossover product ion $\{[(\text{L}^{\text{IPr}_3}\text{-d}_{21}\text{-Cu})(\text{L}^{\text{Bn}_3}\text{-d}_{21}\text{-Cu})(\mu\text{-O})_2](\text{ClO}_4)\}^+$ were observed, thus ruling out equilibration of the compounds with diffusible monomeric species. Reversible loss of O_2 from the (μ -peroxo)dicopper complex also does not occur, as shown by the absence of incorporation of $^{16}\text{O}_2$ (1 atm) into prepared $[(\text{L}^{\text{IPr}_3}\text{-Cu})_2(\mu\text{-}\eta^2\text{:}\eta^2\text{-}^{18}\text{O}_2)](\text{PF}_6)_2$ in CH_2Cl_2 after several days at -80°C (Raman spectroscopy).

(34) Karlin, K. D.; Wei, N.; Jung, B.; Kaderli, S.; Niklaus, P.; Zuberbühler, A. D. *J. Am. Chem. Soc.* **1993**, *115*, 9506–9514.

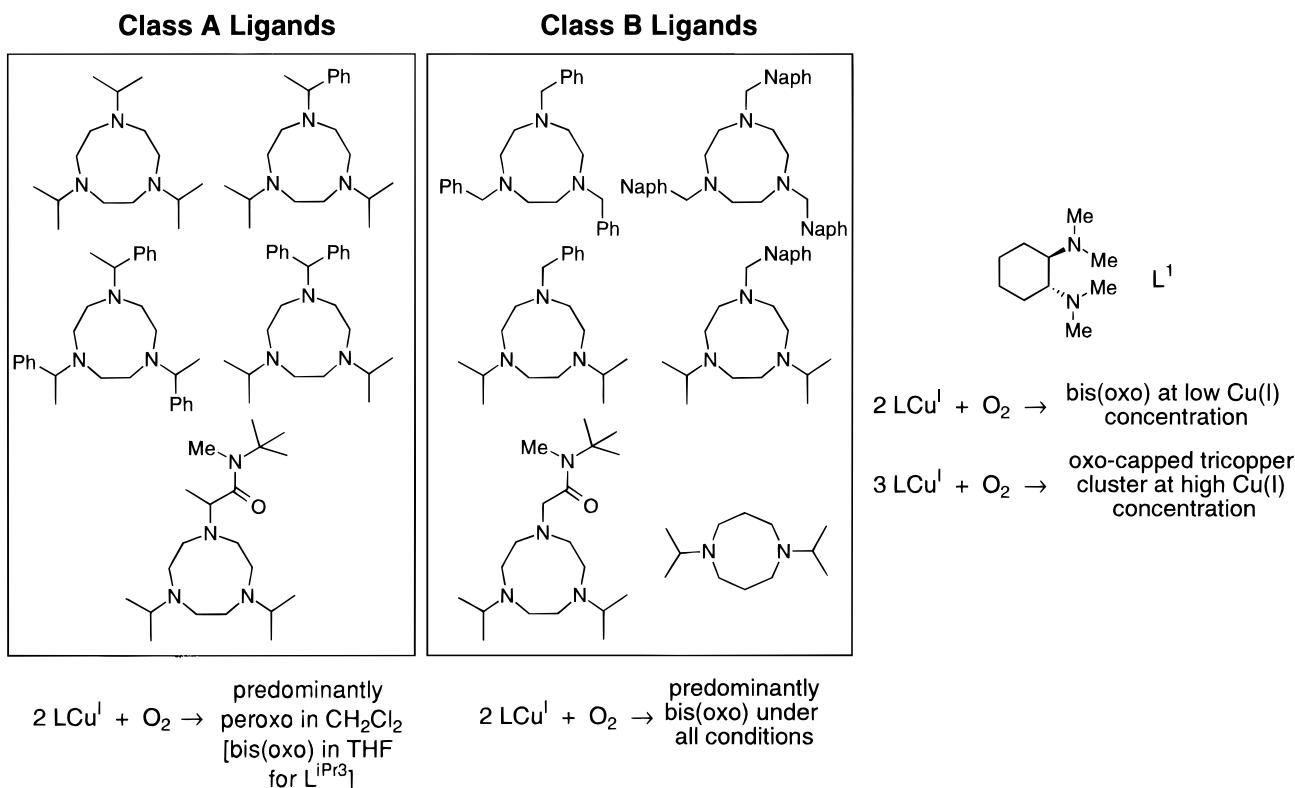


FIGURE 7. Tertiary amine ligands used in low-temperature copper(I)/dioxygen reactions, classified according to the predominant products observed (classes A and B, refs 15, 21, and 37; ligand L^1 , ref 30).

The combined experimental data demonstrate for the first time the reversible scission and formation of the dioxygen O–O bond within a binuclear metal complex. Evidently, when supported by L^{iPr_3} , the two cores $[\text{Cu}_2(\mu\text{-O})_2]^{2+}$ and $[\text{Cu}_2(\mu\text{-}\eta^2\text{:}\eta^2\text{-O})_2]^{2+}$ have similar thermodynamic stabilities and a low activation barrier for interconversion, with the nature of the medium and the counterions being influential in controlling which is the favored oxygenation product. Specifically how different solvents and counterions induce preferential stabilization of the respective isomers is unclear at present. Rationales for the finding of similar stabilities of the two cores and the flat nature of the potential energy surface connecting them have been provided by the results of *ab initio* theoretical calculations wherein $\{[(\text{NH}_3)_3\text{Cu}]_2(\mu\text{-O})_2\}^{2+}$ and $\{[(\text{NH}_3)_3\text{Cu}]_2(\mu\text{-}\eta^2\text{:}\eta^2\text{-O})_2\}^{2+}$ in the gas phase were compared and interconverted.^{21c,32} In brief, although Coulomb forces favor the peroxo over the bis(μ -oxo) form because of the greater distance between the positively charged metal centers, this is counteracted by a nondynamic electron correlation effect involving the LUMO + 1 of the bis(μ -oxo) core (Figure 6). Low-lying in $\{[(\text{NH}_3)_3\text{Cu}]_2(\mu\text{-O})_2\}^{2+}$, this orbital having O–O σ^* character becomes significantly destabilized as the oxygen atoms approach each other to form the $[\text{Cu}_2(\mu\text{-}\eta^2\text{:}\eta^2\text{-O})_2]^{2+}$ core. Large contributions to the ground state wave function from configurations involving occupation of the low-lying LUMO + 1 of the $[\text{Cu}_2(\mu\text{-O})_2]^{2+}$ unit are responsible for the stabilization of this core. In a preliminary assessment of solvent effects, continuum dielectric calculations (using a medium with $\epsilon = 10$) showed that solvation also preferentially stabilizes the bis(μ -oxo) form. Note, however, that specific interactions of the isomeric dications with the first solvent shell or the counterions are not accounted for by this approach.

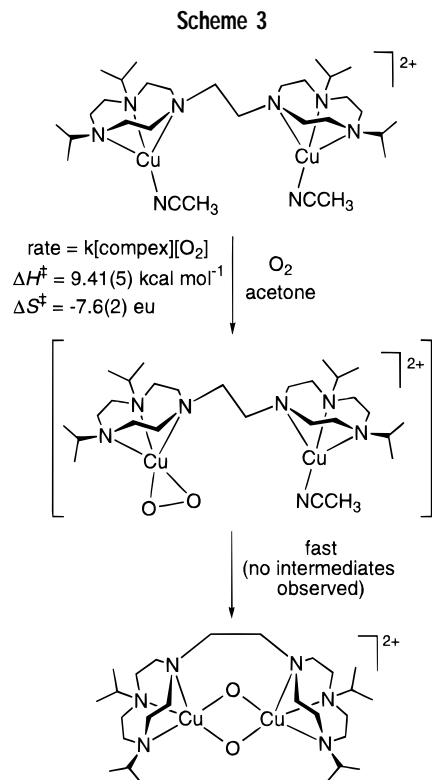
Finally, the Walsh diagram of Figure 6 indicates that the interconversion of the peroxo and bis(μ -oxo) forms involves a continuous diabatic correlation of occupied orbitals along the reaction path, analogous to symmetry-allowed pericyclic reactions in organic chemistry³⁵ and in contrast to the transmutations of so-called bond stretch isomers that have been rationalized by orbital crossings.³⁶

The divergent results of oxygenations of Cu(I) complexes of L^{Bn_3} and L^{iPr_3} indicate that, in addition to solvent and counterion effects, N-donor ligand structure is also an important factor in determining which core topology is favored. The degree of substitution at the carbon α to the N-donors is a key influence, as revealed by a survey^{30,37} of the O_2 reactivity of Cu(I) complexes of the ligands shown in Figure 7 in CH_2Cl_2 or THF. For those tridentate ligands in which every α carbon is tertiary (class A), the peroxo form is favored in CH_2Cl_2 (in the L^{iPr_3} case, the bis(μ -oxo) is favored in THF). If one or more of these α carbons is less substituted (i.e., is secondary or absent, class B), then the bis(μ -oxo) form predominates under all conditions (like L^{Bn_3}). A straightforward steric argument rationalizes the behavior of the complexes of the various ligands; for the class A ligands the hindrance resulting from the three tertiary α carbons inhibits collapse to the contracted $[\text{Cu}_2(\mu\text{-O})_2]^{2+}$ core and allows the larger $[\text{Cu}_2(\mu\text{-}\eta^2\text{:}\eta^2\text{-O})_2]^{2+}$ core to be accessed, an effect that is absent for the smaller class B ligands. Thus, it would appear that the bis(μ -oxo) core is in fact intrinsically favored, with the

(35) Woodward, R. B.; Hoffmann, R. *Conservation of Orbital Symmetry*; Academic Press: New York, 1970.

(36) (a) Stohrer, W.-D.; Hoffmann, R. *J. Am. Chem. Soc.* **1972**, *94*, 779–786. (b) Stohrer, W.-D.; Hoffmann, R. *J. Am. Chem. Soc.* **1972**, *94*, 1661–1668.

(37) Mahapatra, S.; Halfen, J. A.; Berreau, L. M.; Schaller, C.; Tolman, W. B. Unpublished results.



peroxo form only being observable when sufficient steric bulk is provided by the capping ligands to inhibit isomerization to the smaller O–O bond-broken form. For the relatively unhindered, bidentate ligand L^1 studied by Stack and co-workers,³⁰ no peroxo species is ever observed, a bis(μ -oxo)dicopper complex forms at low concentrations of the Cu(I) starting material (≤ 1 mM), and a 3:1 Cu:O₂ reaction to yield an oxo-capped Cu(II)₂Cu(III) complex occurs at high concentrations (≥ 10 mM, Figure 5). Formally, the latter trinuclear species can be viewed to arise from addition of a monomeric Cu(I) unit to a bis(μ -oxo)dicopper(III) core, a reaction that is only possible for a ligand such as L^1 that has reduced steric bulk compared to the other chelates shown in Figure 7.

Control over the course of the oxygenation chemistry can also be effected by the appropriate choice of the tether in binucleating ligands comprised of linked TACN units. For instance, the low-temperature reaction of O₂ with the dicopper(I) complex of 1,2-bis(4,7-diisopropyl-1,4,7-triazol-1-cyclononyl)ethane (*i*-Pr₄dtne) in CH₂Cl₂ or THF yielded a bis(μ -oxo) core only, with no spectroscopic indications for the presence of a peroxo isomer (Scheme 3).³⁸ Stopped-flow kinetics data collected between -90 and $+25$ °C showed that the oxygenation is first order in the concentrations of each of the reagents (dicopper complex and O₂) with activation parameters similar to those seen previously for 1:1 Cu:O₂ reactions.^{21b,34} No intermediates were observed. These results support rate-determining formation of a monocopper–dioxygen adduct followed by fast collapse to a dicopper–dioxygen species and O–O bond cleavage to yield the final bis(μ -oxo) product. An X-ray crystal structure of the complex [(*i*-Pr₄dtne-*d*₂₈)Cu₂(μ -O)₂](SbF₆)₂ revealed a core geometry and C–D⋯O

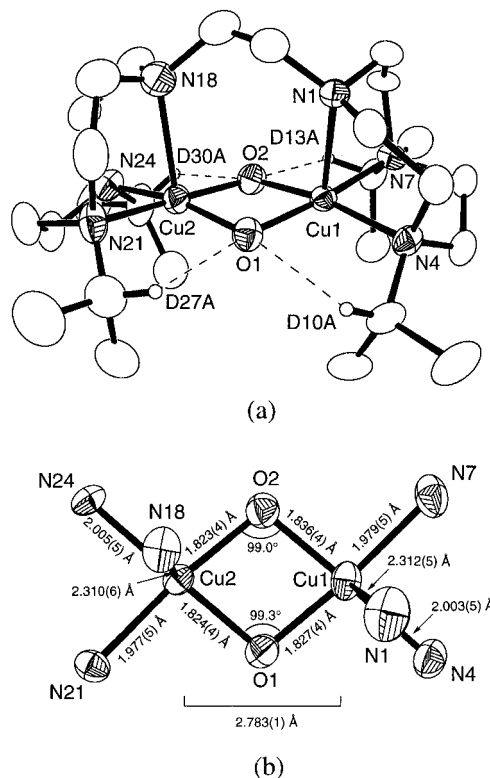


FIGURE 8. (a) X-ray crystal structure of the cationic portion of [(*i*-Pr₄dtne-*d*₂₈)Cu₂(μ -O)₂](SbF₆)₂ and (b) a view of the copper coordination sphere labeled with selected interatomic distances and bond angles.

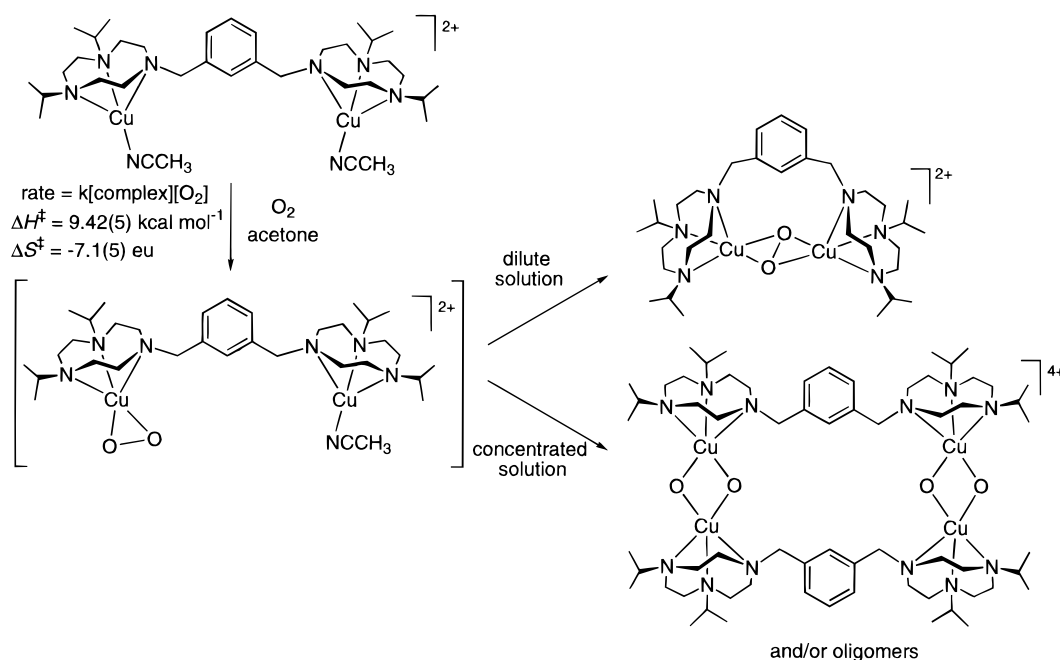
interactions roughly similar to those of the L^{Bn3}-capped analog, but nonetheless different in subtle ways that reflect the influence of the ethylene linker between the macrocycles (Figure 8). Notably, the tether forces the axial N-donors to coordinate in a syn rather than an anti fashion and induces a “puckering” of the Cu₂O₂ rhomb (12° Cu–O1–Cu/Cu–O2–Cu dihedral angle). Despite this distortion, the Cu⋯Cu distance [2.783(1) Å] is similar to that in the L^{Bn3} structure [2.794(2) Å] due to slightly lengthened Cu–O bonds in the *i*-Pr₄dtne case (av 1.83 Å). Similar effects on bis(μ -oxo)dimanganese core geometries have been observed in complexes bridged by additional, relatively small ligands (e.g., acetate, peroxide, or oxide).²⁸

With a more expanded *m*-xylyl linker, interesting complications in the copper–dioxygen chemistry arise because of apparent competition between intra- and intermolecular complex formation (Scheme 4).³⁹ At high concentrations of the dicopper(I) complex of this ligand (≥ 2 mM) in CH₂Cl₂, the reaction with O₂ yields predominantly the bis(μ -oxo) core, but as the concentration of the starting dicopper(I) compound is lowered the relative proportion of peroxo to bis(μ -oxo) increases. These results suggest that an initially formed dioxygen adduct (presumably bound to one metal in the binuclear complex) subsequently partitions between two pathways. The predominant route at low concentration involves intramolecular collapse to yield a (μ -peroxo)dicopper species. Similar species have been reported for other *m*-xylyl-

(38) Mahapatra, S.; Young, V. G., Jr.; Kaderli, S.; Zuberbühler, A. D.; Tolman, W. B. *Angew. Chem., Int. Ed. Engl.* **1997**, *36*, 130–133.

(39) Mahapatra, S.; Kaderli, S.; Llobet, A.; Neuhold, Y.-M.; Palanché, T.; Young, V. G., Jr.; Kaden, T. A.; Que, L., Jr.; Zuberbühler, A. D.; Tolman, W. B. Submitted for publication.

Scheme 4

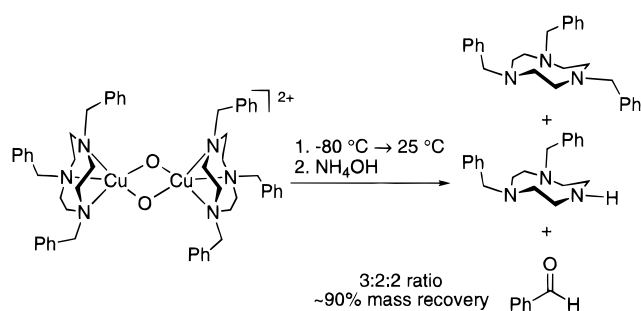


bridged ligand systems with different N-donor caps.⁴⁰ An intermolecular reaction is favored at higher starting material concentrations, yielding “dimer-of-dimer”⁴¹ and/or oligomeric compounds with bis(μ -oxo) cores (Scheme 4). Variable temperature stopped-flow kinetics studies of the oxygenation reaction have been interpreted successfully within this mechanistic framework.³⁹ In sum, by holding the macrocyclic chelates sufficiently far apart, the *m*-xylyl linker inhibits collapse to an intramolecular bis(μ -oxo) adduct and allows formation of a peroxo complex, but only under conditions (low concentration) that disfavor intermolecular chemistry.

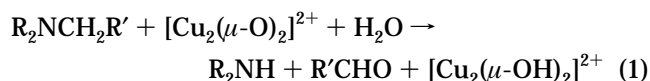
Monoxygenase Reactivity: Decomposition of the Bis(μ -oxo)dicopper Complexes

The peroxo- and bis(μ -oxo)dicopper compounds are thermally unstable and decompose upon warming to give green solutions. Bis(μ -hydroxo)dicopper(II) complexes that differ with respect to the nature of the capping macrocyclic ligand can be crystallized from these solutions, although yields are variable and dependent on the conditions.²¹ In the case of the decompositions of the bis(μ -oxo) complexes capped by L^{Bn_3} and L^{iPr_3} , extraction of Cu(II) from the solutions revealed high overall yields of N-dealkylated ligands and the coproducts acetone and benzaldehyde (cf. results for the L^{Bn_3} case in Scheme 5). For $[(i\text{-Pr}_4\text{dtne})\text{Cu}_2(\mu\text{-O})_2]^{2+}$, N-dealkylation occurred essentially quantitatively and was completely regioselective, affording products derived from cleavage of one isopropyl arm only and none from scission of the ethano linker. On the basis of the results of a labeling experiment wherein

Scheme 5



^{18}O was incorporated into the benzaldehyde isolated from the decay of $[(L^{\text{Bn}_3}\text{Cu})_2(^{18}\text{O})_2]^{2+}$, the decomposition was identified as a monoxygenase reaction (eq 1) analogous to those carried out by various metalloenzymes (e.g., cytochrome P450,^{3a} dopamine β -monoxygenase,^{3f} and secondary amine monoxygenase^{3b}).



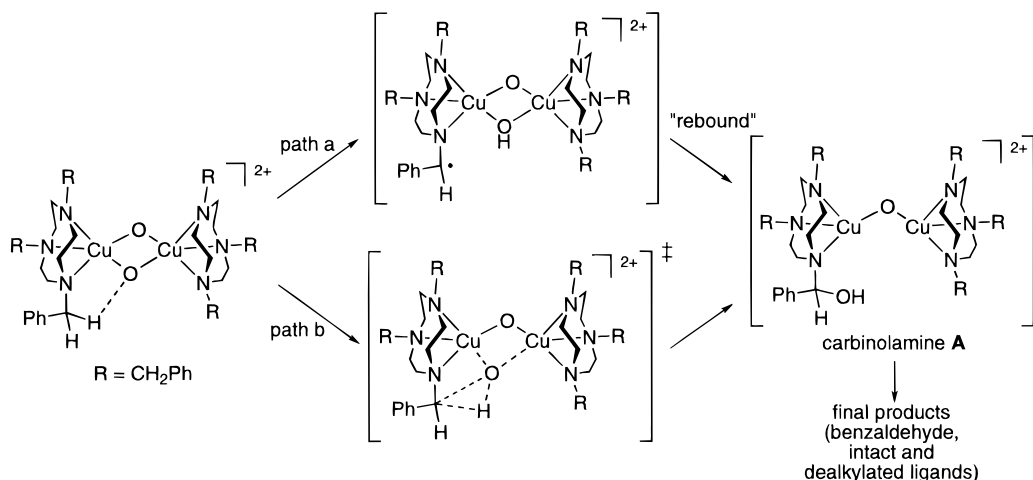
We obtained insight into the mechanism of the decomposition reactions through kinetics and additional isotope labeling experiments.³¹ The reactions of the bis(μ -oxo) compounds are first-order in starting complex concentration and exhibit large kinetic isotope effects (KIEs) upon deuteration at the position α to the ligand N-donor (KIE = $k_{\text{H}}/k_{\text{D}} = 26\text{--}40$ at -40°C). These results show that scission of the $\alpha\text{-C-H(D)}$ bond occurs during the rate-determining step. A significant temperature dependence of the KIEs that is reflected in differences in activation parameters for the protio and deuterio cases implicates tunneling during this C–H bond cleavage process.⁴² A Hammett study in which the rate constants

(40) (a) Cruse, R. W.; Kaderli, S.; Karlin, K. D.; Zuberbühler, A. D. *J. Am. Chem. Soc.* **1988**, *110*, 6882–6883. (b) Karlin, K. D.; Nasir, M. S.; Cohen, B. I.; Cruse, R. W.; Kaderli, S.; Zuberbühler, A. D. *J. Am. Chem. Soc.* **1994**, *116*, 1324–1336.

(41) Related tetranuclear “dimer-of-dimer” complexes of Fe and Mn have been structurally characterized. For example, see: (a) Sessler, J. L.; Sibert, J. W.; Lynch, V. *Inorg. Chem.* **1990**, *29*, 4143–4146. (b) Gultneh, Y.; Ahvazi, B.; Khan, A. R.; Butcher, R. J.; Tuchagues, J. P. *Inorg. Chem.* **1995**, *34*, 3633–3645.

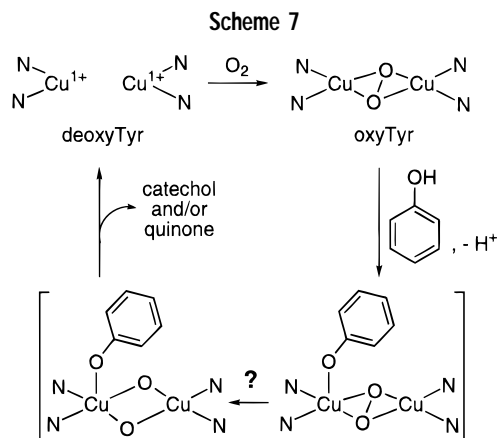
(42) For example, for the decay of the bis(μ -oxo) complex supported by L^{Bn_3} , $\Delta\Delta H^\ddagger = \Delta H^\ddagger_{\text{D}} - \Delta H^\ddagger_{\text{H}} = 2.5 \text{ kcal mol}^{-1}$ and $A_{\text{H}}/A_{\text{D}} = 0.2$. These values are suggestive of a tunneling contribution to the reaction rate; see ref 31 and Kwart, H. *Acc. Chem. Res.* **1982**, *15*, 408–415.

Scheme 6



for decomposition of complexes capped by derivatives of L^{Bn} having various *para*-substituents were plotted versus σ^+ parameters revealed $\rho = -0.8$. This value is similar to those measured for hydrogen atom abstractions from benzylic positions by free radicals,⁴³ as well as for benzylic oxidations by the [Fe=O]³⁺ units in cytochrome P450⁴⁴ and synthetic analogs.⁴⁵ It thus appears that the bis(μ -oxo) core behaves as an electrophilic radical, notwithstanding its diamagnetic, singlet ground state.⁴⁶ Finally, the results of double-labeling and crossover experiments proved that oxygen atom transfer to the α -carbon is an intramolecular process that does not involve diffusible monomeric species.

Taken together, the data are consistent with a mechanism for the decomposition of the bis(μ -oxo) complexes involving intramolecular scission of the α -C–H bond by the intact, electrophilic [Cu₂(μ -O)₂]²⁺ core (Scheme 6). Recall that in the solid state structures of the bis(μ -oxo) complexes interactions between α -C–H(D) bonds and the bridging oxygen atoms are already present. The electrophilic character of the bridging oxo groups also is reflected by the lack of reactivity of the bis(μ -oxo) complexes with strong protic acids, a somewhat surprising finding considering that high oxidation state (μ -oxo)diiron or -dimanganese complexes can be protonated to yield isolable hydroxo-bridged cores.⁴⁷ We speculate that the electrophilicity of the bridging oxygen atoms in the [Cu₂(μ -O)₂]²⁺ core may be traced to the low-lying LUMO + 1 orbital having dominant lobes extending from the bridging oxygen atoms (Figure 6). According to one view of the decomposition reaction, hydrogen atom abstraction from the α -C–H bond by the bridging oxygen atom would generate a carbon-centered radical that is trapped rapidly by the resulting copper–hydroxyl species in a classical



“rebound” pathway (path a, Scheme 6).^{3a} Alternatively (path b), C–H bond scission and O atom transfer may proceed in a concerted, nonsynchronous fashion similar to that suggested recently by Newcomb and co-workers.⁴⁸ Both routes would afford the intermediate carbinolamine A, which would then decompose to the final secondary amine and carbonyl coproducts.

Biological Implications

Despite the current lack of evidence for its existence in a metalloprotein, experimental support for the notion that the bis(μ -oxo)dicopper core may be a reactive intermediate in oxygenase and/or oxidase reactions of multicopper proteins is provided by (i) the synthesis and comprehensive characterization of discrete complexes having this unit, (ii) the direct observation of its formation from a (μ - η^2 : η^2 -peroxo)dicopper precursor, a unit that has been identified in biological systems, and (iii) demonstration of its capability to activate C–H bonds in intramolecular N-dealkylation reactions. For example, in tyrosinase (Tyr), an enzyme that is responsible for the hydroxylation and oxidation of phenols to *o*-quinones, oxygenation of the dicopper(I) active site yields a well-characterized μ - η^2 : η^2 -peroxo species (oxyTyr) analogous to that found in oxyHc (Scheme 7).^{3g,h} One may envision conversion of this intermediate to a bis(μ -oxo) form prior to attack on the phenol substrate. As noted recently,^{3h} whether O–O bond

(43) Russell, G. A. In *Free Radicals*; Kochi, J. K., Ed.; John Wiley & Sons: New York, 1973; Vol. 1, pp 275–331.

(44) Vaz, A. D. N.; Coon, M. J. *Biochemistry* **1994**, *33*, 6442–6449.

(45) Inchley, P.; Smith, J. R. L.; Lower, R. J. *New J. Chem.* **1989**, *13*, 669–676.

(46) For pertinent discussions of the mechanisms of H atom transfer reactions by diamagnetic oxometal reagents, see: (a) Cook, G. K.; Mayer, J. M. *J. Am. Chem. Soc.* **1994**, *116*, 1855–1868. (b) Gardner, K. A.; Mayer, J. M. *Science* **1995**, *269*, 1849–1851.

(47) (a) Que, L., Jr.; True, A. E. *Prog. Inorg. Chem.* **1990**, *38*, 97–200. (b) Kurtz, D. M., Jr. *Chem. Rev.* **1990**, *90*, 585–606. (c) Baldwin, M. J.; Stemmler, T. L.; Riggs-Gelasco, P. J.; Kirk, M. L.; Penner-Hahn, J. E.; Pecoraro, V. L. *J. Am. Chem. Soc.* **1994**, *116*, 11349–11356.

(48) Newcomb, M.; LeTadic-Biadatti, M. H.; Chestney, D. L.; Roberts, E. S.; Hollenberg, P. F. *J. Am. Chem. Soc.* **1995**, *117*, 12085–12091.

scission precedes substrate activation in this way or occurs simultaneously (i.e., the peroxo unit attacks the arene ring directly) is an intriguing unanswered question. Although evidence suggests that hydroxylation of uncoordinated arene units occurs via direct attack of (μ - η^2 : η^2 -peroxo)-dicopper cores in the synthetic analog systems studied to date,^{39,40} there is a need to address the possible role of phenolate coordination to the Tyr active site, perhaps to induce the peroxo \rightarrow bis(μ -oxo) isomerization prior to substrate C–H bond activation (Scheme 7).

Viewed from a broader perspective, the interconversion of the peroxo- and bis(μ -oxo)dicopper complexes is potentially relevant to functional aspects of proteins that contain other metals in their active sites, such as iron or manganese. The involvement of “diamond” [$M_2(\mu$ -O) $_2$] $^{n+}$ cores in biological dioxygen activation and evolution may be a general phenomenon, notable examples including the tetramanganese cluster in the oxygen evolving complex of the photosynthetic apparatus [postulated to contain linked bis(μ -oxo)dimanganese cores],⁷ the reactive form of ribonucleotide reductase [“X”, a diiron(III,IV) unit],⁶ and the species responsible for C–H bond activation in methane monooxygenase [“Q”, proposed to contain a bis(μ -oxo)diiron(IV) core].^{5,6,27} One may draw numerous structural and functional analogies between the synthetic copper species described herein, other diiron model compounds, and these various metalloprotein

active sites.²⁹ Within the current context, we are led by our findings to ask the following question: Might the O–O bond-breaking and -forming reactions that interchange the peroxo and bis(μ -oxo) units in the synthetic copper complexes be important in these metalloproteins? For example, it would appear warranted to reconsider the previously⁴⁹ discounted idea that O–O bond formation in photosynthesis may involve conversion of a bis(μ -oxo)-dimanganese unit to a (μ - η^2 : η^2 -peroxo)dimanganese core.^{7a} The reverse peroxo \rightarrow bis(μ -oxo) isomerization is a reasonable step in the mechanisms of formation of the diiron intermediates Q and X.^{5,6a} Further experimental testing of these hypotheses is needed, as is research oriented toward relating the diverse biological reactivities of the various bis(μ -oxo)dimetal cores to their geometric and electronic structures.

I thank my co-workers and collaborators, listed in the references, who have contributed superbly to this research; their efforts are greatly appreciated. I also thank C. Cramer, B. Smith, J. Halfen, and S. Mahapatra for critical comments and help with the figures. Financial support was provided by the NIH, the NSF, the Searle, Alfred P. Sloan, and Camille & Henry Dreyfus Foundations, and the University of Minnesota.

AR960052M

(49) Proserpio, D. M.; Hoffmann, R.; Dismukes, G. C. *J. Am. Chem. Soc.* **1992**, *114*, 4374–4382.